

# ***PhreshPhish: A Real-World, High-Quality, Large-Scale Phishing Website Dataset and Benchmark***

Thomas Dalton\* Hemanth Gowda Girish Rao Sachin Pargi  
 Alireza Khodabakhshi Joseph Rombs Stephan Jou Manish Marwah\*  
 OpenText

## **Abstract**

Phishing remains a pervasive and growing threat, inflicting heavy economic and reputational damage. While machine learning has been effective in real-time detection of phishing attacks, progress is hindered by lack of large, high-quality datasets and benchmarks. In addition to poor-quality due to challenges in data collection, existing datasets suffer from leakage and unrealistic base rates, leading to overly optimistic performance results. In this paper, we introduce *PhreshPhish*, a large-scale, high-quality dataset of phishing websites that addresses these limitations. Compared to existing public datasets, *PhreshPhish* is substantially larger and provides significantly higher quality, as measured by the estimated rate of invalid or mislabeled data points. Additionally, we propose a comprehensive suite of benchmark datasets specifically designed for realistic model evaluation by minimizing leakage, increasing task difficulty, enhancing dataset diversity, and adjustment of base rates more likely to be seen in the real world. We train and evaluate multiple solution approaches to provide baseline performance on the benchmark sets. We believe the availability of this dataset and benchmarks will enable realistic, standardized model comparison and foster further advances in phishing detection. The datasets and benchmarks are available on Hugging Face (<https://huggingface.co/datasets/phreshphish/phreshphish>).

## **1 Introduction**

Phishing attacks are a pervasive and evolving threat that uses social engineering techniques to deceive millions of Internet users annually. According to the latest Phishing Activity Trends Report [23] released by the Anti-Phishing Working Group (APWG) [6], almost a million phishing attacks were observed just in the fourth quarter of 2024. These attacks are a central component of modern cyber kill chains [51], often involving campaigns that lure users to spoofed websites designed to trick them into revealing sensitive information, such as login credentials and financial data. The data thus obtained often serves as an initial entry point to fraud, identity theft and large-scale data breaches, resulting in substantial financial and reputational damage. In 2023 alone, phishing contributed significantly to the estimated \$12.5 Billion in cyberfraud losses reported to the FBI [20].

Phishing remains a popular attack vector due to its effectiveness, low cost, and ease of deployment. A major contributing factor is the widespread availability of phishing kits [11, 7]. These kits contain complete phishing websites in a ready-to-deploy package, and can often be downloaded for free or even purchased on the dark web markets [35], making such attacks accessible even to unskilled adversaries.

Despite considerable research efforts, detecting phishing sites remains a challenging task [13]. Various approaches have been proposed to detect phishing, including use of blacklists, whitelists,

---

\*Equal contribution.

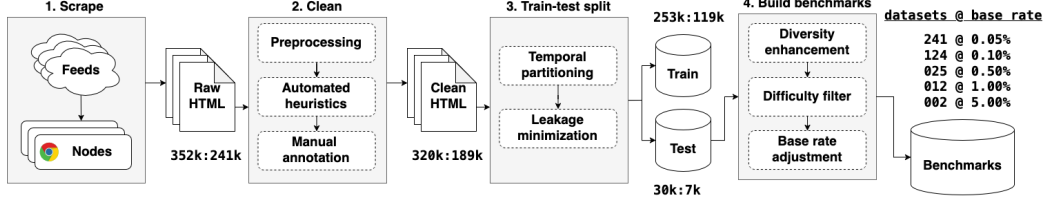


Figure 1: Our end-to-end pipeline consists of four distinct stages and we show the benign-to-phishing count at each step: (1) benign and phishing HTML is collected from the web using a real browser to ensure high fidelity; (2) the retrieved HTML is cleaned and assessed for quality using a combination of automated heuristics and human annotation; (3) train and test splits are created temporally and pruned to minimize leakage; (4) benchmark datasets are created by applying a set of diversity, difficulty and base rate filters.

heuristic-based techniques and machine learning methods. However, its adversarial nature, with attackers constantly adapting to avoid detection, and lack of good quality data undermines these defense approaches. Phishing websites are typically short-lived, highly dynamic, and often employ techniques such as obfuscation, cloaking [54], and fast-flux hosting [37].

Deployed phishing detection systems can be integrated into various applications, with browser plugins serving as a convenient option for verifying websites, and blocking phishing sites before users access them. To be effective in real-world settings, such systems must satisfy two key desiderata — **(1) Low number of false positives:** legitimate websites should only be rarely, if ever, blocked, implying a high precision,  $P(W|A)^2$ , where  $1 - P(W|A)$  represents the proportion of incorrectly blocked sites; and **(2) Low latency:** detection must operate in near real time, ideally within a few hundred milliseconds, to minimize user disruption.

State-of-the-art machine learning-based phishing detection systems can be categorized into two broad approaches: **(1) Direct phishing detection**, where models are trained to classify webpages directly as phishing or benign [50, 36, 47, 3]. These models rely on feature extraction or representation learning from a (partially) labeled dataset of webpages. **(2) Target brand-based phishing detection**, where models are trained to identify the brand a webpage attempts to mimic, and phishing is inferred from inconsistencies between the webpage’s URL and the legitimate URLs associated with the identified brand [2, 31, 29]. While the latter approach does not require a dataset of phishing webpages, it relies on a curated set of target brands, and typically incurs much higher detection latency.

While the collection of large-scale web datasets is itself nontrivial, successfully scraping phishing pages—which behave adversarially to avoid detection—presents its own set of unique challenges beyond those typically encountered in general web scraping. In addition to the fact that the modern web is increasingly **dynamic**, issues such as **ephemerality**, **cloaking**, and **staleness** significantly complicate the collection of high-quality datasets which may be used to train and evaluate phishing detection models. These challenges necessitate the development of robust methodologies for collecting, cleaning, and validating phishing datasets to ensure their quality and utility for research purposes. We believe that these obstacles, discussed in greater detail in Section 3.1, contribute to the overall lack of high-quality datasets in this area. Although a search for publicly available phishing datasets would appear to yield promising results, we observed substantial quality issues with many datasets (see Appendix B). We also could not find any suitable benchmark datasets that facilitated a robust comparative evaluation of detection techniques despite the significant role that phishing plays in cybercrime.

In this work, we present *PhreshPhish*, a large-scale, high-quality phishing website dataset collected over several months. To the best of our knowledge, this is the largest publicly available phishing website data and offers significantly higher quality compared to other such public datasets. Further, we create realistic benchmark datasets for comparison between detection methods. Figure 1 provides a schematic of the entire data pipeline from obtaining the phishing and benign URLs to finally producing the training, test and benchmark datasets.

To summarize, we make the following key contributions:

<sup>2</sup> $W$  indicates a true phishing website;  $A$  is a phishing website identified by a model.

- Publicly release *PhreshPhish*, a large-scale, high-quality phishing website dataset, that addresses drawbacks of existing such datasets. Unlike prior datasets, our dataset is (1) larger-scale; (2) higher quality; (3) more recent (with planned periodic versioned updates).
- We also release a suite of benchmark datasets to standardize the evaluation of detection methods. These benchmarks span 5 different base rates, ranging from 0.05% to 5%, making them more representative of real-world settings; further, we employ filters to increase dataset difficulty and diversity, and minimize data leakage.
- We evaluate and compare a number of baseline methods on our benchmark dataset to demonstrate the utility of our dataset and benchmarks. We also provide a detailed analysis of the performance of these methods, including their strengths and weaknesses, and discuss the implications for future research in this area.

## 2 Related Work

### 2.1 Phishing datasets

While an internet search for phishing website datasets returns a large number of hits, the actual number of datasets of a substantial size containing both URL and raw HTML data are very few. Most such datasets only contain website URLs, but no HTML (see Appendix B); others contain phishing emails or texts. A few datasets on Kaggle [9, 15, 34, 14] and Hugging Face [16, 17] contain raw HTML, however these are either smaller datasets or several years old; further, the quality of these datasets is generally poor, and they either do not create a test or benchmark dataset, or those datasets are randomly generated leading to leakage from the training data.

### 2.2 Minimizing data leakage

Most approaches to splitting a dataset into a training and a test set assume the data to be i.i.d. and perform a random split. A common exception is time-series data, where “future” data points are usually used for testing. However, data leakage [25] can still occur due to other factors. Kapoor et al. [24] provide a taxonomy of data leakage in machine learning, including cases where training and test data are not independent. A typical example is when multiple data points are collected from the same entity, such as a patient [40], where random splitting can place data from the same entity in both sets, causing leakage. When entities are easily identifiable, data can be split to avoid overlap. In phishing detection, one potential source of leakage is sites built using the same kit. However, since such information is usually not available, we adopt a simple approach: we directly compare test and training points for similarity, dropping test points that are too similar to any training point. To make this search scalable to a large dataset, we use locality sensitive hashing [4].

### 2.3 Phishing detection approaches

One useful way to categorize phishing detection systems is by their deployment mode: (1) real-time, interactive detection – that blocks users from accessing harmful sites; and (2) offline detection – for generating blacklists and whitelists. The former imposes strict latency constraints, making computationally intensive methods or those requiring features that are slow to retrieve unsuitable for use. Our dataset is primarily designed to support the real-time detection scenario.

Phishing detection approaches have evolved over time [48, 55, 27], with early ones based on blacklists and whitelists of URLs. Although fast and effective for known sites, this approach suffers from complexity of maintaining these dynamic lists and its inability to detect zero-day phishing attacks. Subsequent methods used rules and heuristics based on features, which were later leveraged for machine learning models. The features can be broadly categorized into three types: (1) URL-based, (2) HTML-based, and (3) host-based.

URL-based features refer to lexical features derived from the entire URL or its components [32, 33]. Since URLs contain strong discriminative signals and are relatively short, a large number of datasets and methods focus solely on URLs-based features for detection [19]. HTML-based features are extracted from the HTML of a page, including its content, structure (DOM tree), tags, embedded links, and its visual rendering [36]. Host-based features relate to *where* a website is hosted and include its IP address, domain name properties, geographic information, and similar attributes [32].

Due to their retrieval latency, these features are less suitable for real-time detection scenarios, which typically require response times under a few hundred milliseconds. Since our dataset is focused more towards real-time detection, it excludes host-based features.

A wide range of machine learning approaches have been applied to phishing detection, spanning from hand-crafted features to learning representations of raw inputs. While many methods aim to directly classify phishing pages [50], others have focused on identifying the impersonated brand first, usually using webpage snapshots and a reference dataset of known brands, followed by checking URL consistency [2, 1, 31, 29]. Most recently, LLMs are being used for detecting phishing pages [28, 26, 8, 53]. LLMs now have large enough context sizes that an entire HTML page can fit. Although they are computationally expensive, large datasets or model training is not required.

### 3 PhreshPhish Dataset

We collected our dataset over eight months (July 2024 to March 2025), encompassing a broad range of phishing and benign URLs. Phishing URLs were primarily sourced from PhishTank [44], the AntiPhishing Working Group (APWG) eCrime eXchange [18], and NetCraft [38]. Benign URLs were drawn from anonymized browsing telemetry from over six million global Webroot users and Google search results for heavily targeted brands. These user-sourced URLs provide a more realistic and representative sample of benign pages that users are likely to encounter on the web as opposed to those from other datasets such as Common Crawl [12]. The dataset was cleaned and curated to ensure that it is of high quality and free from noise and other issues that are common in other datasets.

#### 3.1 Scraping challenges

Despite substantial research in web crawling, gathering data for applications in security remains difficult, particularly for phishing detection, due to its evasive and transient nature. Below, we outline key challenges and our mitigation strategies.

Table 1: Common failure modes encountered when scraping phishing webpages.

Failure Mode	Description
Takedown Notice	Host (e.g., Cloudflare) has removed the page and displays a standard "page removed" or takedown banner.
Cloaking	Malicious domain now redirects to a benign or unrelated page, sometimes to avoid detection.
CAPTCHA	Page requires solving a CAPTCHA, preventing automated scraping. This primarily applies to legitimate pages but is increasingly used by phishing pages as a cloaking strategy.
JavaScript-Heavy Page	Critical content is loaded dynamically via JavaScript and is not captured by traditional crawlers.
HTTP Errors (4xx/5xx)	Page returns error codes like 404 (Not Found), 403 (Forbidden), or 500 (Internal Server Error).
Geofencing or IP Block	Page returns alternate content or blocks access based on the IP region or blacklists scrapers.

**Dynamic pages** Modern websites frequently rely on JavaScript frameworks like React [46] and Angular [5] to load content dynamically. This poses a challenge for traditional crawlers, which only fetch static HTML and cannot execute client-side scripts. Consequently, dynamic content is often missed, limiting the usefulness of datasets such as Common Crawl and datasets derived from it [45, 43, 10], which rely on traditional scraping tools like Apache Nutch [39].

**Ephemerality** Phishing pages are often short-lived and may be taken down before they can be scraped. This is particularly true for pages that are hosted on compromised benign domains, which are often taken down by the domain owner or hosting provider. This can lead to situations where the scraper is unable to access the original phishing page and instead is presented with a benign page or a takedown notice. This is a common failure mode that is frequently encountered when scraping phishing pages in particular.



**Cloaking** Cloaking [54] is a technique used by attackers to present different content conditioned on specific criteria, such as a client’s IP address or user agent. This can lead to situations where the scraper is presented with a benign page instead of the phishing page, resulting in mislabeled data. This is a particularly pernicious problem that can lead to model poisoning [49].

**Staleness** Phishing techniques and tactics constantly evolve, with new pages and campaigns emerging regularly. In addition, underlying web technologies change over time, with new standards like HTML5 and frameworks like GraphQL [21] being adopted. Datasets must be regularly updated to reflect the current state of the web and of modern phishing techniques. Many existing phishing datasets are outdated and no longer relevant, as they were collected years ago and do not reflect the current state of the web. To combat the issue of staleness, we plan to maintain *PhreshPhish* with regular updates to ensure its relevance and utility for research purposes.

### 3.2 Our scraping process

To address the challenges outlined above, we developed a scraping pipeline that is designed to maximize the probability of capturing high-quality phishing data. Our scraping pipeline leverages Selenium [22] to render pages in full browser instances, capturing dynamic content missed by traditional tools. Pages are scraped using a distributed cluster running Windows and Chrome, allowing us to address the challenges of dynamic pages and cloaking. Nodes in the cluster are configured to use a variety of user agents and IP addresses to improve the chances of capturing the phishing page. To mitigate the ephemerality challenge, URLs are scraped within minutes of being reported to our feeds. Finally, we continuously monitor the performance of our scraping system and make adjustments as needed to ensure that it remains effective.

### 3.3 Cleaning process

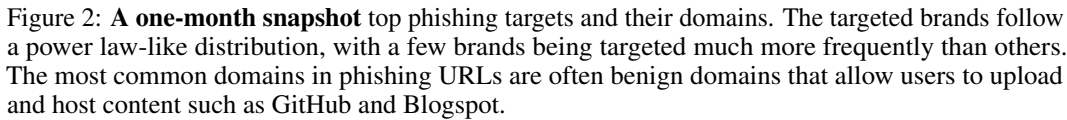
Although our scraping process is designed to maximize the probability of capturing phishing data, bad data corresponding to one of the failure modes described in Table 1 is still common. After the raw data is collected, it undergoes a cleaning process to further improve data quality. This cleaning process is a combination of automated and manual steps where a number of heuristics are used to remove low-quality data.

Because URLs are often reported to multiple feeds, we normalize the URL to a canonical form and deduplicate the data at the URL level. The canonicalization process includes removing trailing slashes and converting the URL to lowercase<sup>3</sup>. Next, the HTML is parsed and the title of the page is extracted. Pages with titles containing certain keywords such as *"forbidden"* or *"not found"* are removed as they are likely to be scrape failures.

Pages are then grouped together and a representative page, known as a prototype, is selected from each group for manual inspection. A human annotator inspects the prototypical page and decides whether to keep or remove the page from the dataset. The decision is then applied to all nearest neighbors of the prototype with respect to cosine similarity of the TF-IDF features of the page. This process continues until a specified budget (i.e. the maximum number of prototypes to inspect) is exhausted. To maximize the efficiency of the cleaning process, we use two distinct grouping schemes. The first grouping is done by performing locality-sensitive hashing (LSH) via random projection. The second grouping is done with respect to the page title. The groupings are then ordered from largest to smallest with the largest groups being inspected first. Although the cleaning stage requires manual human inspection and annotation, it is optimized to an extent due to the fact that the human annotator only needs to inspect a representative page from each group and any decision made about the prototypical page is applied to all nearest neighbors in bulk. This significantly reduces the amount of manual work required to clean the dataset. Furthermore, a budget is imposed on the number of prototypes to be inspected to ensure that the cleaning process is efficient and does not take an excessive amount of time. Pages likely to contain personally identifiable information (PII) are also removed from the dataset. Further details including pseudocode for cleaning and our PII removal process are provided in Appendix C.

<sup>3</sup>Although URLs can contain uppercase letters, we convert it to lowercase for deduplication purposes only since it is often the case that the same URL will be reported multiple times, occasionally with different casing. After deduplication, the original case-sensitive URL is retained.

The final dataset is comprised of approximately 253k benign and 119k phishing pages, totaling 372k data points in all. Further details and exploratory analysis on the final dataset are provided in Appendix C.



*For better or for worse, benchmarks shape a field.*  
—David Patterson, 2017 Turing award winner [41]

In contrast to our approach, we found most publicly available phishing website datasets either lack a test or benchmark dataset, or suffer from significant training-to-test set leakage, leading to inflated performance evaluation. Further, the base rate in most datasets is too high to serve as realistic benchmarks.

Starting from the clean dataset, we first perform temporal partitioning, followed by leakage filtering to remove test data points that show high similarity to any point in the train set. The pseudocode to generate the test set is shown in Algorithm 2 in Appendix D.

**Leakage filter** While temporal separation provides some protection against data leakage from the train to the test set, very similar points could still exist between train and test datasets. To mitigate this problem, we traverse the test set and discard points whose TF-IDF cosine distance is less than a

specified threshold from any train points. LSH is used to make searching the train set more scalable. Figure 5 in Appendix D shows the temporal distribution of the train and test data sets based on date of collection.

## 4.2 PhreshPhish Benchmarks

To encourage the development of more robust and generalizable phishing detection models, we provide a suite of benchmark datasets. The benchmark datasets are derived from the test dataset but are further processed to make them more challenging and representative of real-world scenarios. The steps to create the benchmarks are shown in Algorithm 3 in Appendix D.

**Diversity enhancement** We prune as well as augment the test dataset to make it more diverse and representative. We augment the benign data points with points corresponding to the top targeted brands. The targeted brands distribution is estimated from the phishing test data, and benign URLs are obtained using Google search. Similarly, one can augment the dataset with pages corresponding to top industry categories.

Many data points have dissimilar URLs but very similar HTMLs. We prune such phishing data points from the test set. This is implemented similar to the leakage filter but with the test set and only the HTML is compared.

**Difficulty filter** Applying the difficulty filter prunes out “easy” points, making the dataset more challenging to classify. There are several approaches to discovering easy points including exploring various data features, determining the most confounding feature values for the output classes, and selecting data points with those values. We take a simpler approach and assume the classification probability of a correctly classified data point can be taken as a proxy of its difficulty. We run the test set through a classifier trained on the training set. Correctly classified phishing points with score greater than  $1 - \delta$  are considered easy and candidates for pruning. We randomly sample and drop  $k\%$  of the entire dataset. Specifically, we set  $\delta = 0.15$ , and  $k = 10$ . While we currently sample the candidates uniformly, an alternate approach would be to assign weights to the entire test set based on their scores, with higher weights for “easier” points, and then perform weighted sampling over the entire set. Figure 3 shows impact of applying the difficulty filter on performance.

**Base rate adjustment** The base rate of phishing points in our test set is about 33%. Other publicly available test datasets have similar high base rates. However, in practice the base rates a detector observes are much lower, and vary depending on a multitude of factors including data provenance and the model pipeline used in deployment. To represent a wide range of scenarios, we create a large number of benchmark datasets with varying base rates. In particular, we create benchmark datasets with five different base rates varying from 0.05% to 5%. To account for variance, multiple instances,  $m$ , are sampled for each base rate, resulting in 404 total datasets. For lower base rates, the number of phishing points in a benchmark set are miniscule, and hence the variance is high.

*Determining  $m$ :* How many instances,  $m$ , are required, given a base rate,  $b$ , corresponding to  $k$  phishing points in a dataset of size  $N$ , for the model error estimate,  $M_e$ , to be accurate within a margin of error  $e$  (e.g.,  $\pm 1\%$ )? Since model error is an average, we can assume  $M_e \sim \mathcal{N}(\mu_{M_e}, \sigma_{M_e})$  (per central limit theorem).  $m$  is sufficiently large when  $m \geq \frac{z^2 \cdot \sigma_{M_e}^2}{e^2}$  where  $\sigma_{M_e}^2$  is the empirical variance of the model error and  $z$  is the standard normal z-score corresponding to a desired confidence level. For each  $b$ , we sample multiple small sets of instances to compute average empirical variance, which is then used to estimate  $m$ . This analysis assumes sampling with replacement; sampling without replacement generally requires fewer samples, however, the difference is negligible when  $k \ll N$ , as is true in our case. Another advantage of sampling without replacement is that all available points are covered. In our experiments, we adopt sampling without replacement with  $m$ ’s higher than the estimated lower bound with 1% margin of error and 95% confidence level. The base rates and the corresponding  $m$ ’s in the benchmark datasets are: 0.05% (241), 0.1% (124), 0.5% (25), 1% (12), 5% (2).

As shown in Figure 3, model performance is highly sensitive to the base rate, with performance improving as the base rate increases. Importantly, most of the strong performance results reported in the literature on this task can be largely attributed to the use of unrealistically high base rates.

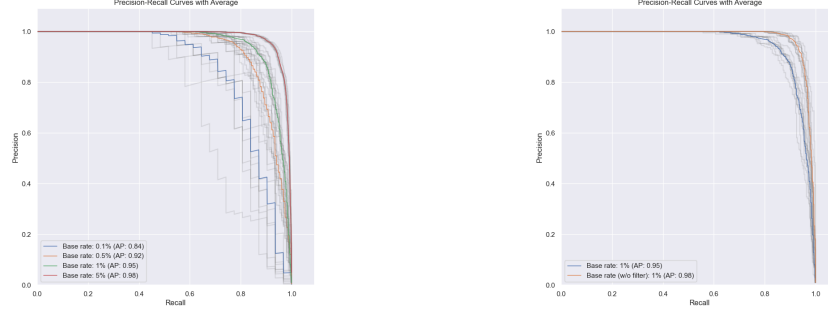


Figure 3: Left: Precision-recall curves on the benchmark datasets. Right: Precision-recall curves on benchmark datasets with and without applying the difficulty filter

## 5 Baseline Models

Phishing detection is a binary classification problem where the input space  $\mathcal{X}$  is the Cartesian product  $\mathcal{X} = \mathcal{U} \times \mathcal{H}$  where  $\mathcal{U}$  denotes the space of URLs and  $\mathcal{H}$  denotes the space of HTML content<sup>4</sup>. The goal is to learn a function  $f : \mathcal{U} \times \mathcal{H} \rightarrow [0, 1]$  that estimates the conditional probability  $P(Y = 1|x)$ , where  $Y \in \{0, 1\}$  is the binary class label (with  $Y = 1$  indicating a phishing page and  $Y = 0$  indicating a benign page) and  $x = (u, h) \in \mathcal{X}$ . The function is learned from a labeled dataset  $\mathcal{D} = \{(x_i, y_i)\}_{i=1}^N$ .

We implemented several representative approaches for real-time phishing detecting, including: (1) a linear model trained on n-gram and hand-crafted features; (2) a shallow feedforward neural network (FNN) using the same feature set; (3) a BERT-based model with a classifier head fine-tuned on raw HTML and URLs; and, (4) a large language model (LLM) used in a zero-shot prediction setting. For the linear and FNN models, input features include tokenized character-level n-grams from both the URL and HTML content, as well as hand-engineered features such as the length of the URL, number of nodes in the HTML DOM tree, and other domain-specific features. In contrast, the BERT and LLM-based approaches operate directly on raw textual inputs to learn rich representations. Our objective is not to optimize for state-of-the-art performance, but rather to establish baseline results on the benchmark datasets using common solution approaches. Model architecture and training details for each approach are described in Appendix E.

**Linear model** The linear model is a simple linear classifier  $f(x) = W \cdot x + b$  implemented using LinearSVC from the scikit-learn library [42] where parameters  $W$  and  $b$  are learned by minimizing the L2-regularized squared hinge loss:  $\mathcal{L}(W, b) = \frac{1}{N} \sum_{i=1}^N (\max(0, 1 - y_i(W \cdot x_i + b)))^2 + \frac{\lambda}{2} \|W\|_2^2$ .

**FNN model** The FNN model uses the same input representation as the linear model but replaces the linear scoring function with a shallow neural network comprising of a single hidden layer with 32 neurons and ReLU activation. Input features are binarized and subject to frequency-based feature selection to reduce dimensionality. The model outputs a scalar probability estimate  $f(x) = \sigma(W_2 \cdot \text{ReLU}(W_1 \cdot x + b_1) + b_2)$ . This architecture introduces a small amount of non-linearity while maintaining tractable training and inference costs. Training is performed using binary cross-entropy loss with the Adam optimizer at a learning rate of 0.001.

**BERT-based feature learning** In this approach, we tokenize the raw, concatenated URL  $u \in \mathcal{U}$  and HTML  $h \in \mathcal{H}$  and input to a BERT-based encoder model, which generates a hidden contextualized representation,  $\mathbf{h} = \text{Encoder}(\text{tokenize}(u \oplus h)) \in \mathbb{R}^{n \times d}$ , where  $n$  is the number of tokens and  $d$  is encoder model dimension. In particular, we use the `gte-large` pre-trained embedding model [30], which computes the dense embedding as  $x = \frac{1}{n} \sum_{i=1}^n h_i \in \mathbb{R}^d$ . We attach a linear classification head for phishing detection,  $f(x) = \sigma(W \cdot x + b) \in [0, 1]$ . We fully fine-tune the model using a binary cross-entropy loss for two epochs on the training dataset.

**LLM-based prediction** We prompt an LLM with a webpage URL and its processed HTML to produce a rating indicating the likelihood that the page is a phishing site. The prompt is zero-shot,

<sup>4</sup>Other input modalities such as host-based features (i.e. domain age, SSL certificate validity, etc.) could be used as well but we exclude them here since their inclusion tends to introduce latency that would be unacceptable for real-time detection.

and the HTML is pruned to remove non-informative elements such as JavaScript, CSS and comments, inspired by [26]. This reduces input tokens and filters out content that is likely to be irrelevant to phishing detection. The returned rating is normalized and perturbed with small Gaussian noise to enable construction of a smooth precision-recall curve. Due to cost considerations and goal of establishing baseline performance, we use a smaller, earlier-generation model: gpt-4o-mini. We expect a larger, state-of-the-art reasoning LLM would produce improved performance. Further details, including the full prompt, are provided in Appendix E.

## 5.1 Results comparison and discussion

Users downstream of phishing detection systems are typically highly sensitive to false positives – instances where access to legitimate websites may be blocked. This is quantified by precision, the fraction of times users are correctly blocked. Consequently, commercial products aspire to a very high value of precision while also maintaining a good recall. Accordingly, we evaluate our models on two performance measures – the average precision, which is an approximation of the area under the precision-recall curve and the precision at a recall of 0.9.

We evaluate the models on the test dataset and the benchmark datasets for the five base rates. As expected, most models perform well on the test data set, which has a base rate of 18.3%. Table 2 summarizes the results for the four models. For each base rate, results are averaged over all corresponding benchmarks datasets. We find performance drops significantly as the base rate decreases. Overall, the GTE model performs the best. More evaluation results, including precision-recall curves and confusion matrices at multiple threshold values, are provided in Appendix E.

Model		0.05	0.10	0.50	1.0	5.0	18.3 (full)
Linear	AP	0.5712 $\pm$ 0.0118	0.6592 $\pm$ 0.0134	0.8277 $\pm$ 0.0089	0.8745 $\pm$ 0.0052	0.9502 $\pm$ 0.0004	0.9940
	P@R=0.90	0.1232 $\pm$ 0.0173	0.2039 $\pm$ 0.0312	0.4179 $\pm$ 0.0528	0.5349 $\pm$ 0.0300	0.8684 $\pm$ 0.0111	0.9510
FNN	AP	0.2395 $\pm$ 0.0097	0.3512 $\pm$ 0.0100	0.6415 $\pm$ 0.0104	0.7367 $\pm$ 0.0094	0.8787 $\pm$ 0.0025	0.9546
	P@R=0.90	0.0347 $\pm$ 0.0065	0.0625 $\pm$ 0.0115	0.1374 $\pm$ 0.0156	0.2176 $\pm$ 0.0357	0.6224 $\pm$ 0.0123	0.9035
GTE	AP	0.7771 $\pm$ 0.0128	0.8142 $\pm$ 0.0101	0.8958 $\pm$ 0.0067	0.9236 $\pm$ 0.0065	0.9715 $\pm$ 0.0002	0.9918
	P@R=0.90	0.2222 $\pm$ 0.0296	0.3118 $\pm$ 0.0364	0.5666 $\pm$ 0.0353	0.7099 $\pm$ 0.0461	0.9322 $\pm$ 0.0034	0.9855
LLM	AP	0.0223 $\pm$ 0.0012	0.0367 $\pm$ 0.0018	0.1306 $\pm$ 0.0061	0.2248 $\pm$ 0.0085	0.5552 $\pm$ 0.0139	0.7976
	P@R=0.90	0.0062 $\pm$ 0.0005	0.0123 $\pm$ 0.0012	0.0450 $\pm$ 0.0108	0.0690 $\pm$ 0.0138	0.2690 $\pm$ 0.0451	0.7780

Table 2: Mean average precision (AP) and mean precision at recall = 0.90 for each benchmark base rate, broken out by model. Values are reported as mean  $\pm$  error, where the error reflects the maximum absolute deviation from the 95% bootstrap confidence interval.

## 6 Conclusions

We introduced *PhreshPhish*, which to the best of our knowledge, constitutes the largest, highest-quality public corpus of phishing websites available. Existing phishing website datasets often suffer from low quality due to the inherent challenges of scraping phishing websites. To address this, we implemented a robust scraping pipeline and then systematically post-processed the collected data to eliminate invalid and mislabeled samples (see Algorithm 1 in Appendix C). We also minimized train-test leakage (see Algorithm 2 in Appendix D), another concern with existing datasets. Most published work on phishing detection report excellent results – primarily due to use of unrealistically high base rates. As expected, we found that model performance degrades sharply as the base rate decreases to more realistic values. To enable more realistic evaluation of phishing models, we constructed  $\sim 400$  benchmark datasets with real-world base rates ranging from 0.05% to 5%, while also increasing task difficulty and diversity (see Algorithm 3 in Appendix D). Our evaluation of common detection approaches on the benchmark datasets shows significant room for improvement. Given the importance of false positives on user experience, we adopt average precision and precision@recall=R as key performance metrics. We make our dataset and benchmarks publicly available on Hugging Face. The code used to scrape and process the dataset, construct the test and benchmark datasets, and to build and evaluate the baseline models is publicly available on Github <https://github.com/phreshphish/phreshphish>. Finally, to keep the dataset fresh, we plan to release versioned datasets and benchmarks periodically.

## References

- [1] Sahar Abdelnabi, Katharina Krombholz, and Mario Fritz. Visualphishnet: Zero-day phishing website detection by visual similarity. In *Proceedings of the 2020 ACM SIGSAC conference on computer and communications security*, pages 1681–1698, 2020.
- [2] Sadia Afroz and Rachel Greenstadt. Phishzoo: Detecting phishing websites by looking at them. In *2011 IEEE fifth international conference on semantic computing*, pages 368–375. IEEE, 2011.
- [3] Ali Aljofey, Qingshan Jiang, Abdur Rasool, Hui Chen, Wenyin Liu, Qiang Qu, and Yang Wang. An effective detection approach for phishing websites using url and html features. *Scientific Reports*, 12(1):8842, 2022.
- [4] Alexandr Andoni and Piotr Indyk. Near-optimal hashing algorithms for approximate nearest neighbor in high dimensions. *Communications of the ACM*, 51(1):117–122, 2008.
- [5] Angular. <https://angular.dev>. Accessed: 2025-04-19.
- [6] Anti-Phishing Working Group (APWG). <https://apwg.org/about-us/>. Accessed: 2025-04-20.
- [7] Hugo Bijmans, Tim Booi, Anneke Schwedersky, Aria Nedgabat, and Rolf van Wegberg. Catching phishers by their bait: Investigating the dutch phishing landscape through phishing kit detection. In *30th USENIX security symposium (USENIX security 21)*, pages 3757–3774, 2021.
- [8] Tri Cao, Chengyu Huang, Yuexin Li, Wang Huilin, Amy He, Nay Oo, and Bryan Hooi. Phishagent: a robust multimodal agent for phishing webpage detection. In *Proceedings of the AAAI Conference on Artificial Intelligence*, volume 39, pages 27869–27877, 2025.
- [9] Phishing Website HTML Classification. <https://www.kaggle.com/datasets/huntingdata11/phishing-website-html-classification>. Accessed: 2025-04-20.
- [10] Data Commons. <https://datacommons.org>. Accessed: 2025-05-19.
- [11] Marco Cova, Christopher Kruegel, and Giovanni Vigna. There is no free phish: An analysis of "free" and live phishing kits. *WOOT*, 8:1–8, 2008.
- [12] Common Crawl. <https://commoncrawl.org>. Accessed: 2025-04-17.
- [13] Avisha Das, Shahryar Baki, Ayman El Aassal, Rakesh Verma, and Arthur Dunbar. Sok: a comprehensive reexamination of phishing research from the security perspective. *IEEE Communications Surveys & Tutorials*, 22(1):671–708, 2019.
- [14] Phishing Data. <https://www.kaggle.com/datasets/aljofey/phishing-data>. Accessed: 2025-04-20.
- [15] Crawling2024(Phishing Websites Dataset). <https://www.kaggle.com/datasets/haozhang1579/crawling2024>. Accessed: 2025-04-20.
- [16] Phishing Dataset. <https://huggingface.co/datasets/ealvaradob/phishing-dataset>. Accessed: 2025-04-20.
- [17] Phishing Detection Dataset. [https://huggingface.co/datasets/huynq3Cyradar/Phishing\\_Detection\\_Dataset](https://huggingface.co/datasets/huynq3Cyradar/Phishing_Detection_Dataset). Accessed: 2025-04-20.
- [18] eCrime eXchange. <https://apwg.org>. Accessed: 2025-03-28.
- [19] Ayman El Aassal, Shahryar Baki, Avisha Das, and Rakesh M Verma. An in-depth benchmarking and evaluation of phishing detection research for security needs. *Ieee Access*, 8:22170–22192, 2020.
- [20] FBI - Internet Crime Complaint Center (IC3). 2023 ic3 annual report. <https://www.ic3.gov/AnnualReport/Reports>, 2024. [Online; accessed 2025-04-20].

- [21] GraphQL. <https://graphql.org>. Accessed: 2025-04-19.
- [22] Selenium Grid. <https://www.selenium.dev/documentation/grid/>. Accessed: 2025-03-27.
- [23] Anti-Phishing Working Group. Phishing attack trends report – 2024 q4. <https://apwg.org/trendsreports/>, 2025. [Online; accessed 2025-04-20].
- [24] Sayash Kapoor and Arvind Narayanan. Leakage and the reproducibility crisis in ml-based science. *arXiv preprint arXiv:2207.07048*, 2022.
- [25] Shachar Kaufman, Saharon Rosset, Claudia Perlich, and Ori Stitelman. Leakage in data mining: Formulation, detection, and avoidance. *ACM Transactions on Knowledge Discovery from Data (TKDD)*, 6(4):1–21, 2012.
- [26] Takashi Koide, Hiroki Nakano, and Daiki Chiba. Chatphishdetector: Detecting phishing sites using large language models. *IEEE Access*, 2024.
- [27] Wenhao Li, Selvakumar Manickam, Yung-Wey Chong, Weilan Leng, and Priyadarsi Nanda. A state-of-the-art review on phishing website detection techniques. *IEEE Access*, 2024.
- [28] Yuexin Li, Chengyu Huang, Shumin Deng, Mei Lin Lock, Tri Cao, Nay Oo, Hoon Wei Lim, and Bryan Hooi. {KnowPhish}: Large language models meet multimodal knowledge graphs for enhancing {Reference-Based} phishing detection. In *33rd USENIX Security Symposium (USENIX Security 24)*, pages 793–810, 2024.
- [29] Yuexin Li, Hiok Kuek Tan, Qiaoran Meng, Mei Lin Lock, Tri Cao, Shumin Deng, Nay Oo, Hoon Wei Lim, and Bryan Hooi. Phishintel: Toward practical deployment of reference-based phishing detection. *arXiv preprint arXiv:2412.09057*, 2024.
- [30] Zehan Li, Xin Zhang, Yanzhao Zhang, Dingkun Long, Pengjun Xie, and Meishan Zhang. Towards general text embeddings with multi-stage contrastive learning. *arXiv preprint arXiv:2308.03281*, 2023.
- [31] Yun Lin, Ruofan Liu, Dinil Mon Divakaran, Jun Yang Ng, Qing Zhou Chan, Yiwen Lu, Yuxuan Si, Fan Zhang, and Jin Song Dong. Phishpedia: A hybrid deep learning based approach to visually identify phishing webpages. In *30th USENIX Security Symposium (USENIX Security 21)*, pages 3793–3810, 2021.
- [32] Justin Ma, Lawrence K Saul, Stefan Savage, and Geoffrey M Voelker. Beyond blacklists: learning to detect malicious web sites from suspicious urls. In *Proceedings of the 15th ACM SIGKDD international conference on Knowledge discovery and data mining*, pages 1245–1254, 2009.
- [33] Justin Ma, Lawrence K Saul, Stefan Savage, and Geoffrey M Voelker. Learning to detect malicious urls. *ACM Transactions on Intelligent Systems and Technology (TIST)*, 2(3):1–24, 2011.
- [34] Malicious and Benign Website dataset. <https://www.kaggle.com/datasets/jackcavar/malicious-and-benign-website-dataset>. Accessed: 2025-04-20.
- [35] Simon Migliano. The dark web is democratizing cybercrime. <https://hackernoon.com/the-dark-web-is-democratizing-cybercrime75e951e2454>, August 2018. [Online; accessed 2025-04-20].
- [36] Rami M Mohammad, Fadi Thabtah, and Lee McCluskey. Phishing websites features. *School of Computing and Engineering, University of Huddersfield*, 138, 2015.
- [37] Thomas Nagunwa, Paul Kearney, and Shereen Fouad. A machine learning approach for detecting fast flux phishing hostnames. *Journal of information security and applications*, 65:103125, 2022.
- [38] Netcraft. <https://www.netcraft.com>. Accessed: 2025-03-28.
- [39] Apache Nutch. <https://nutch.apache.org/>. Accessed: 2025-04-16.

- [40] Mustafa Umit Oner, Yi-Chih Cheng, Hwee Kuan Lee, and Wing-Kin Sung. Training machine learning models on patient level data segregation is crucial in practical clinical applications. *medRxiv*, pages 2020–04, 2020.
- [41] David Patterson. For better or worse, benchmarks shape a field. *Communications of the ACM*, 55, 2012.
- [42] F. Pedregosa, G. Varoquaux, A. Gramfort, V. Michel, B. Thirion, O. Grisel, M. Blondel, P. Prettenhofer, R. Weiss, V. Dubourg, J. Vanderplas, A. Passos, D. Cournapeau, M. Brucher, M. Perrot, and E. Duchesnay. Scikit-learn: Machine learning in Python. *Journal of Machine Learning Research*, 12:2825–2830, 2011.
- [43] Guilherme Penedo, Hynek Kydlíček, Loubna Ben allal, Anton Lozhkov, Margaret Mitchell, Colin Raffel, Leandro Von Werra, and Thomas Wolf. The fineweb datasets: Decanting the web for the finest text data at scale. In A. Globerson, L. Mackey, D. Belgrave, A. Fan, U. Paquet, J. Tomczak, and C. Zhang, editors, *Advances in Neural Information Processing Systems*, volume 37, pages 30811–30849. Curran Associates, Inc., 2024.
- [44] PhishTank. <https://phishtank.org>. Accessed: 2025-03-28.
- [45] Colin Raffel, Noam Shazeer, Adam Roberts, Katherine Lee, Sharan Narang, Michael Matena, Yanqi Zhou, Wei Li, and Peter J Liu. Exploring the limits of transfer learning with a unified text-to-text transformer. *Journal of machine learning research*, 21(140):1–67, 2020.
- [46] React. <https://react.dev>. Accessed: 2025-04-19.
- [47] Vahid Shahrivari, Mohammad Mahdi Darabi, and Mohammad Izadi. Phishing detection using machine learning techniques. *arXiv preprint arXiv:2009.11116*, 2020.
- [48] Lizhen Tang and Qusay H Mahmoud. A survey of machine learning-based solutions for phishing website detection. *Machine Learning and Knowledge Extraction*, 3(3):672–694, 2021.
- [49] Zhiyi Tian, Lei Cui, Jie Liang, and Shui Yu. A comprehensive survey on poisoning attacks and countermeasures in machine learning. *ACM Computing Surveys*, 55(8):1–35, 2022.
- [50] Colin Whittaker, Brian Ryner, and Marria Nazif. Large-scale automatic classification of phishing pages. In *Ndss*, volume 10, page 2010, 2010.
- [51] Wikipedia contributors. Cyber kill chain — Wikipedia, the free encyclopedia. [https://en.wikipedia.org/w/index.php?title=Cyber\\_kill\\_chain&oldid=1256319774](https://en.wikipedia.org/w/index.php?title=Cyber_kill_chain&oldid=1256319774), 2024. [Online; accessed 6-April-2025].
- [52] Lixia Xie, Hao Zhang, Hongyu Yang, Ze Hu, and Xiang Cheng. A scalable phishing website detection model based on dual-branch tcn and mask attention. *Computer Networks*, 263:111230, 2025.
- [53] Jun Zhang, Peiqiao Wu, Jeffrey London, and Dan Tenney. Benchmarking and evaluating large language models in phishing detection for small and midsize enterprises: A comprehensive analysis. *IEEE Access*, 2025.
- [54] Penghui Zhang, Adam Oest, Haehyun Cho, Zhibo Sun, RC Johnson, Brad Wardman, Shaown Sarker, Alexandros Kapravelos, Tiffany Bao, Ruoyu Wang, Yan Shoshitaishvili, Adam Doupe, and Gail-Joon Ahn. Crawlphish: Large-scale analysis of client-side cloaking techniques in phishing. In *2021 IEEE Symposium on Security and Privacy (SP)*, pages 1109–1124, 2021.
- [55] Rasha Zieni, Luisa Massari, and Maria Carla Calzarossa. Phishing or not phishing? a survey on the detection of phishing websites. *IEEE Access*, 11:18499–18519, 2023.



## A *PhreshPhish* Datasheet

Motivation	Purpose	To further anti-phishing research, particularly web-based phishing. One of the primary challenges of web-based phishing detection is that it is difficult to obtain high-quality, real world phishing datasets and we hope that this dataset and benchmark will help to spur more innovation and research in the field.
	Creators	OpenText, Inc. fully funded and created the dataset.
Composition	Description	Dataset is comprised of HTML webpage data, labels, and metadata in Parquet format.
	Sample Instance	<pre> {   "sha256": "0b7244604505e864d5d836...",   "url": "https://login-gemini-homep...",   "label": "phishing",   "target": "gemini",   "date": "2025-03-02",   "lang": "en",   "lang_score": 0.893,   "html": "&lt;html&gt;...&lt;/html&gt;" }</pre>
	Count	About 372k samples: 253k benign pages and 119k phishing pages.
	Splits	Train and test splits are provided as well as 404 benchmarks created from the test split.
Collection Process	Acquisition	The data was acquired by scraping the HTML contents located at a URL. URLs were sourced from various phishing and benign feeds.
	Time Frame	The data was scraped over the course of 8 months, between July 2024 and March 2025.
Data Processing	Description	The raw data underwent the following steps: (1) URL deduplication; (2) cleaning as described in Section 3; (3) Train/test split and benchmark creation as described in Section 4.
	Code Availability	All code is available on Github <a href="https://www.github.com/phreshphish/phreshphish">https://www.github.com/phreshphish/phreshphish</a> .
Usage Considerations	Intended Usage	This dataset should be used to further anti-phishing research.
	Cautions	Because the URLs were sourced, in part, from customer use traces, some of the corresponding webpages may contain questionable content including pornographic and/or hateful speech.
	Limitations	Although effort was made to ensure the dataset is of high quality, due to the size it is impossible to fully validate that low-quality samples have been fully removed.
Distribution	License	The dataset is made available under the Creative Commons Attribution 4.0 International license.
	Hosting	The full dataset is publicly available on Hugging Face <a href="https://huggingface.co/datasets/phreshphish/phreshphish">https://huggingface.co/datasets/phreshphish/phreshphish</a> .
	Maintenance	We plan to periodically release updates to the dataset as new phishing URLs are discovered.

## B Existing Datasets

We searched for phishing datasets on common dataset hosting sites such as Hugging Face and Kaggle. On each of these sites, we searched for the terms "*phishing*" and "*phish*". On Hugging Face, we restricted the search to datasets with more than 10K rows. On Kaggle, we restricted the search to datasets larger than 100 MB in size. Almost all datasets we found were either URL-only or related to email phishing, with only a few containing both raw HTML webpage and URL data.

Table 3: Phishing datasets on common hosting sites

Repository	Total	Feature type		
		URL only	Email	URL & HTML
Hugging Face	35	15	14	2
Kaggle	19	6	4	4
Harvard Dataverse	2	0	2	0
OpenML	4	2	1	0
UCI ML Repo	3	3	0	0

### B.1 Data Quality

In this section, we provide a quality assessment of two datasets found on Kaggle: Aljofey [3] and Crawling2024 [15]. Our goal is to demonstrate that these exhibit substantial quality issues and therefore motivate the need for a new, high-quality dataset. We apply the same cleaning methodology used for constructing our own dataset, using rejection rates from manual inspection as a proxy for data quality. Specifically, we apply: (1) URL normalization and deduplication; (2) removal of samples with titles indicative of scrape failure (Table 4); (3) grouping based on TF-IDF features using LSH and manual inspection of the groups; and (4) grouping by title and manual inspection of the most common titles. To make the comparisons feasible across datasets, we set a budget of 60 LSH bins and 50 distinct titles: approximately one hour of work for a human annotator. High rejection rates among the inspected samples suggests that poor quality is not confined to edge cases but is pervasive. We summarize the results of our quality assessment in Table 5.

Table 4: Keywords used for filtering bad titles. These keywords are used to automatically identify and remove low-quality samples from the dataset.

Keywords	Example title
"400"	"400 Bad Request"
"403"	"403 Forbidden"
"404"	"404 Not Found"
"410"	"410 Gone"
"found"	"Page not found!"
"encontrada"	"Página não encontrada"
"forbidden"	"Access Forbidden"
"error"	"Sorry, an error occurred"
"suspended"	"Account Suspended"
"bad request"	"Bad Request"
"cloudflare"	"Cloudflare Anti-Bot"
"just a moment"	"Just a moment..."
"warning!   there might be a problem"	"Warning!   There might be a problem with the requested link"
"url shortener, branded short"	"URL Shortener, Branded Short Links & Analytics   TinyURL"
"denied"	"Access Denied"

Because a complete manual inspection is not feasible, we estimate a lower and upper bound for the amount of data that would remain were cleaning to continue to completion. The upper bound is a generous estimate of the number of samples that would remain after cleaning and is equal to the number in row labeled "After Stage 2" in Table 5. The lower bound is, we believe, a more realistic estimate of the number of samples that would remain after cleaning and is equal to the upper bound multiplied by the rejection rate observed in the manual inspection of the LSH bins and titles. The

Table 5: Two-stage cleaning pipeline results for three datasets. Stage 1 applies automated filtering; Stage 2 applies manual inspection using two grouping schemes: LSH and title. Note: Some examples were removed by multiple filters, so removal counts may overlap and not sum to exact totals.

Step	Aljofey			Crawling2024			PhreshPhish (ours)		
	Phish	Benign	Total	Phish	Benign	Total	Phish	Benign	Total
<i>Stage 0: Initial Size</i>									
Initial Size	27,280	32,972	60,252	26,687	29,428	56,115	118,752	253,189	371,941
<i>Stage 1: Automated Filtering</i>									
URL Duplicates	2,936	129	3,065	1,069	166	1,235	0	0	0
HTML Missing	1,843	1,103	2,946	1,427	103	1,530	0	0	0
Bad Title	12,715	5,018	17,733	6,322	665	6,987	0	0	0
<b>After Stage 1</b>	<b>12,722</b>	<b>26,851</b>	<b>39,573</b>	<b>18,938</b>	<b>28,660</b>	<b>47,598</b>	<b>118,752</b>	<b>253,189</b>	<b>371,941</b>
<i>Stage 2: Manual Inspection</i>									
LSH Rejections	2,530	5,422	7,952	3,390	3,470	6,860	331	80	411
Title Rejections	794	183	977	555	47	602	447	27	474
<b>After Stage 2</b>	<b>9,398</b>	<b>21,246</b>	<b>30,644</b>	<b>14,993</b>	<b>25,143</b>	<b>40,136</b>	<b>117,974</b>	<b>253,082</b>	<b>371,056</b>
<b>Total Removed</b>	<b>17,882</b>	<b>11,726</b>	<b>29,608</b>	<b>11,694</b>	<b>4,285</b>	<b>15,979</b>	<b>778</b>	<b>107</b>	<b>885</b>
<b>Rejection Rate (%)</b>	<b>65.5%</b>	<b>35.6%</b>	<b>49.1%</b>	<b>43.8%</b>	<b>14.6%</b>	<b>28.5%</b>	<b>0.65%</b>	<b>0.04%</b>	<b>0.24%</b>

rejection rate is calculated as the number of samples removed divided by the total number of samples in the dataset.

**Aljofey, et al. [3]** This dataset contains 60k samples, with 27k labeled as phishing and 33k labeled as benign. We found that this dataset contained a large number of data points that could immediately be removed under our automated filtering process (the majority of which were due to having bad titles such as "404 Not Found"). After running our cleaning process, over 65% of the phishing samples in this dataset were removed, leaving only 9,398 phish samples remaining in the dataset. The benign samples were also heavily affected, with 35% of the benign samples being removed.

Assuming the remaining un-inspected samples are perfectly clean, the dataset would contain 9,398 phishing samples and 21,246 benign samples. Under more realistic assumptions and based on rejection rates observed, however, we estimate that the dataset would contain only around 3,242 phishing samples and 13,682 benign samples if cleaning were to continue to completion.

**Crawling2024 [52]** This dataset contains 56k samples, with 27k labeled as phishing and 29k labeled as benign. Although this dataset performed better than Aljofey, there was still a significant amount of data that was removed after applying our cleaning process.

Assuming the remaining un-inspected samples are perfectly clean, the dataset would contain 14,993 phishing samples and 25,143 benign samples. Under more realistic assumptions and based on rejection rates observed, however, we estimate that the dataset would contain only around 8,400 phishing samples and 20,000 benign samples if cleaning were to continue to completion.

**PhreshPhish (ours)** Our dataset contains 372k samples, with 119k labeled as phishing and 253k labeled as benign. Because we had already applied the cleaning process to our own dataset, the automated filtering stage didn't result in any new samples being removed. After applying the manual inspection process, we found only a few hundred samples needing removal. This is expected and we do not claim that our dataset is free from all errors as an unlimited cleaning budget is not feasible. However, we believe the significantly lower rejection rates in our dataset compared to the other two datasets shows that our dataset is of much higher quality.

## C Our Dataset

### C.1 Cleaning details

Following the data collection phase, we conducted a dedicated cleaning stage to address residual noise, failure modes, and inconsistencies not resolved by the scraping pipeline alone. While our browser-based scraper was designed to mitigate many of the challenges associated with phishing

data collection (e.g., cloaking, ephemeral content), scraping artifacts and systemic noise remained common, particularly among phishing pages. Representative examples of these artifacts are shown in Figure 4.

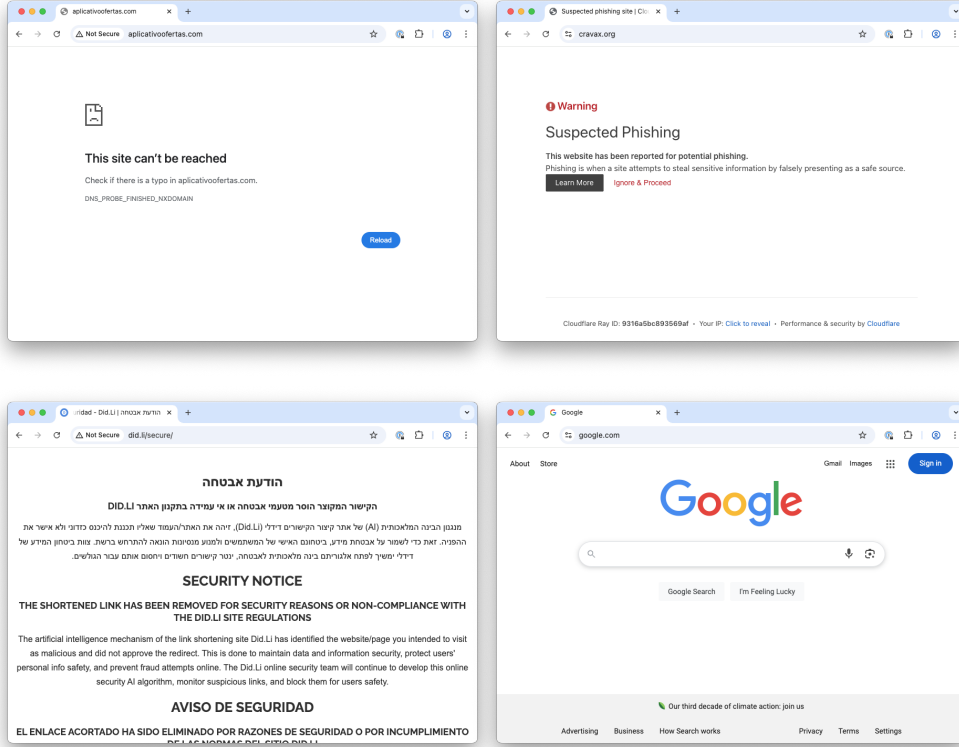


Figure 4: Multiple failure modes are frequently encountered when scraping phishing pages. **Top Left:** DNS resolution issues can prevent the page from being scraped. **Top Right:** Security takedown notices can prevent the page from being scraped. **Bottom Left:** URL shortening services will sometimes block access to the intended page. **Bottom Right:** Redirects to the legitimate target brand page can occur resulting in mislabeled data.

Our approach to dataset cleaning, described in Algorithm 1, is based on the idea of using a combination of two different grouping strategies to quickly identify and remove pages that are likely to correspond to a failure mode. Pages are first vectorized using TF-IDF features (line 4). These vectors are then projected into binary hash bins using random projection to form coarse similarity groups (lines 5 and 9). Pages are also grouped by their HTML `<title>` tags (lines 7 and 10), which is helpful for identifying pages that are likely to be derived from the same template or boilerplate code. Within each group, a single representative (prototype) page is selected and presented for manual inspection (lines 18 and 19). The human annotator is then asked to determine whether the page reflects a failure mode or otherwise invalid content (line 20). If the page represents a scrape failure, it and all of its nearest neighbors (under cosine similarity in the TF-IDF space) are removed from the dataset (line 21). Groups are prioritized by size, ensuring that the cleaning budget is spent efficiently (lines 16 and 17).

## C.2 Handling PII

We focused our PII removal efforts on the benign class only as this is the class that is most likely to contain sensitive information. In fact, because phishing pages are often designed to look like legitimate pages, they often contain data such as phone numbers and email addresses which may be useful signals for phishing detectors.

Query parameters in the URL are often used to pass sensitive information such as user IDs, session tokens, and other PII to the server and are therefore removed from the URL. We also removed data

---

**Algorithm 1** Cleaning process

---

```
1: Input: Dataset  $\mathcal{D}$ , budget  $b$ 
2: Output: Cleaned dataset  $\mathcal{D}' \subseteq \mathcal{D}$ 
3:
4:  $X \leftarrow \text{TFIDF}(\mathcal{D})$  ▷ create TF-IDF features
5:  $B \leftarrow (X \cdot \mathcal{N}(0, 1)) \geq 0$  ▷ bin via random projection
6:
7:  $T \leftarrow \{\text{GetTitle}(x) \mid x \in \mathcal{D}\}$ 
8:
9:  $G_B \leftarrow \text{GroupBy}(B, X)$  ▷ group by LSH bins
10:  $G_T \leftarrow \text{GroupBy}(T, X)$  ▷ group by titles
11:
12: // iterate through groups, keeping track of which pages to remove
13:  $R \leftarrow \emptyset$  ▷ to remove
14: for  $G \in \{G_B, G_T\}$  do
15:    $i \leftarrow 0$  ▷ stop when budget exhausted
16:   while  $i < b$  do
17:     for  $g \in \text{Sorted}(G, \text{key} = |g|, \text{descending} = \text{True})$  do
18:        $p \leftarrow \text{SelectPrototype}(g)$ 
19:        $\text{doRemove} \leftarrow \text{ManualInspect}(p)$ 
20:       if  $\text{doRemove}$  then
21:          $R \leftarrow R \cup \text{GetNearestNeighbors}(p)$ 
22:       end if
23:        $i \leftarrow i + 1$ 
24:     end for
25:   end while
26: end for
27: return  $\mathcal{D}' \leftarrow X \setminus R$ 
```

---

points with URLs that may contain customer information. This is done by first transforming the URL into a string of words by replacing special characters (e.g. / and -) with spaces and then using a DistilBERT-based NER model<sup>5</sup> to identify any URLs that contain a person’s name. We then used SmolLM2-1.7B-Instruct<sup>6</sup> to determine whether the name identified by the NER model is a well-known or otherwise public figure or not. If the name is not a well-known or public figure, the URL and corresponding page is removed from the dataset.

We did not attempt to remove other PII such as email addresses or phone numbers from the benign class as this would require differentiating between true PII and data that is not PII but looks like it (e.g. a customer support phone number or email address). Websites that tend to contain true PII (e.g. social media sites) contain such data behind authentication walls. Because our scraping process does not attempt to log in to sites, we do not expect truly sensitive data to be present in the dataset.

### C.3 Risks and limitations

We found that additional kinds of data including screenshots and raw network traffic (to detect things like redirects, for example) could be useful for both cleaning as well as for training other kinds of models (e.g. reference-based image models) and hope to include these features in future versions of the dataset. Because there are varying degrees of sophistication in phishing campaigns, there is a risk that the phishing pages we were able to scrape are systemically easier to scrape (and therefore to detect) than those that are not included in the dataset.

Finally, while our primary intent is to support research in phishing detection and web security, we acknowledge the dual-use risk of releasing this dataset. Malicious actors could theoretically use the dataset to refine and improve their tactics. However, we believe that openness and transparency is ultimately more beneficial to the community than secrecy. By making the dataset and benchmarks available, we aim to foster the development of stronger defenses against phishing attacks.

---

<sup>5</sup><https://huggingface.co/dslim/bert-base-NER>

<sup>6</sup><https://huggingface.co/HuggingFaceTB/SmolLM2-1.7B-Instruct>

## C.4 Summary of selected dataset facets

Table 6: Summary statistics for selected URL features.

Feature	Description	Min		25%		50%		75%		Max	
		Phish	Benign	Phish	Benign	Phish	Benign	Phish	Benign	Phish	Benign
URL length	Num characters in the URL	14	8	83	44	40	58	57	78	2,544	1,199
Domain length	Num characters in domain	1	1	6	6	7	9	10	12	60	43
Path length	Num characters in the path	3	32	1	19	3	32	16	52	2,073	981
Subdomain length	Num characters in subdomain	0	0	4	3	11	3	17	3	92	63

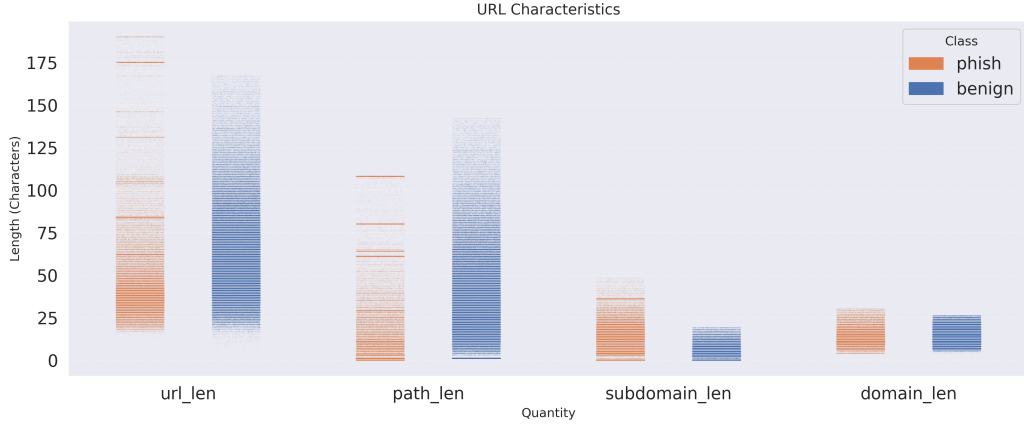


Figure 6: Distribution of URL characteristics.

Table 7: Summary statistics for selected HTML features.

Feature	Description	Min		25%		50%		75%		Max	
		Phish	Benign	Phish	Benign	Phish	Benign	Phish	Benign	Phish	Benign
HTML length	<html> tag lengths	42	23	69.66	65,320.75	38,400	180,243	126,522	409,249	39,544,635	57,863,340
Head tag length	Sum of all <head> tag lengths	13	13	1,267	9,435	6,218	40,352	17,902	118,630	25,817,150	30,385,165
Image tag length	Sum of all <img> tag lengths	6	6	84	116	148	155	311	258	25,817,150	1,454,356
Script tag length	Sum of all <script> tag lengths	17	17	92	108	165	204	311	597	2,257,807	13,280,918

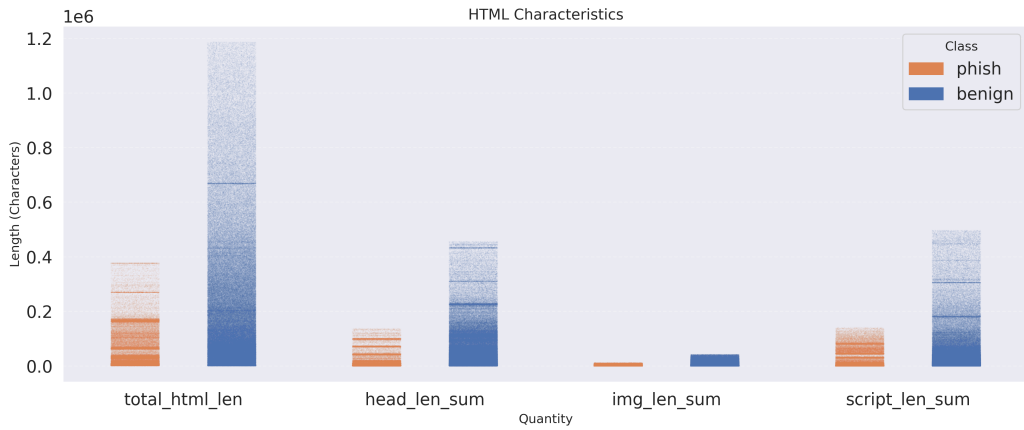


Figure 7: Distribution of HTML characteristics.

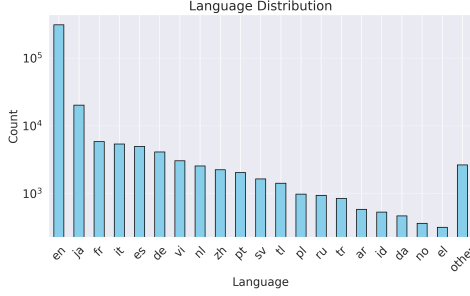


Figure 8: Distribution of languages in the dataset.

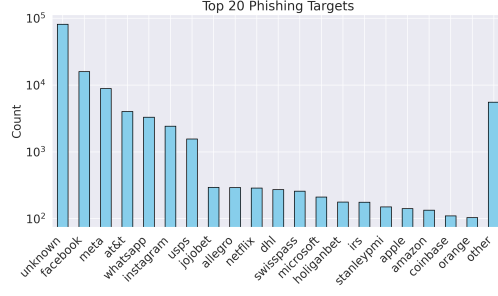


Figure 9: Top phishing targets.

## D Test and Benchmark Sets

Figure 5 provides a temporal view of the dataset after the cleaning process, aggregated at a daily granularity. The volume of phishing data collected each day depended primarily on the number of phishing pages reported by the feeds, as well as occasional local infrastructure issues. In contrast, the benign data collection shows greater variability, partly because benign URLs are more readily available – allowing a large number to be collected in a single day – and also because benign pages tend to be less dynamic and remain fresh for longer periods than phishing pages. This accounts for the periods during which no benign data was collected.

Algorithm 2 outlines the main procedure used to split the dataset into training and test sets. A test split fraction,  $p = 0.7$  was used. Lines 4–7 create a temporal split, performed in a stratified manner to preserve class proportions across both sets. However, due to differences in data collection between phishing and benign, the temporal separation between train and test occur at different times for the two classes as shown in Figure 5.

Lines 10–19 minimize data leakage from training set to the test set by iterating over the test dataset, searching for similar instances in the training set using LSH, and removing test points with similarity above a threshold.

Algorithm 3 outlines the procedure for creating the benchmark datasets from the test set. Lines 5–6 describe the process of enhancing test dataset diversity. The benign part of the test set is augmented with legitimate websites corresponding to the top target phishing brands (determined from the training phishing set). For the phishing test data, pairwise comparisons are performed, and one sample from each pair of highly similar instances is removed. This pruning step eliminates highly similar samples, increasing the diversity of the phishing dataset.

Lines 9–13 describe the difficulty filter, where a fraction of randomly selected “easy” points, defined by highly confident correct scores predicted by a model, are discarded. We use  $\delta = 0.15$ , and  $k = 10\%$ .

Lines 16–24 describe the rate adjustment procedure, where for each of five base rates, the number of phishing points ( $numPhish$ ) and instances ( $numInstances$ ) are determined, and subsequently for each base rate  $numInstances$  samples of size  $numPhish$  are sampled without replacement from the reduced phishing test set, obtained from the previous step (difficulty filter).

---

**Algorithm 2** Train-test split

---

```
1: Input:  $\mathcal{D}$  (clean dataset),  $p$  (test set fraction),  $\tau$  (similarity threshold)
2: Output:  $\mathcal{D}_{train}$  (train set),  $\mathcal{D}_{test}$  (test set)
3:
4: // temporal partition
5:  $\mathcal{D} \leftarrow \text{SortByTime}(\mathcal{D})$ 
6:  $\mathcal{D}_{train} \leftarrow \{\mathcal{D}_{1:k} \mid k = \lfloor (1-p) * |\mathcal{D}| \rfloor\}$ 
7:  $\mathcal{D}'_{test} \leftarrow \mathcal{D} \setminus \mathcal{D}_{train}$ 
8:
9: // minimize leakage
10:  $\text{lsh} \leftarrow \text{ConstructLSH}(\mathcal{D}_{train})$ 
11:  $\mathcal{D}_{test} \leftarrow \emptyset$ 
12: for  $x \in \mathcal{D}'_{test}$  do
13:   candidates  $\leftarrow \text{lsh.search}(x)$ 
14:   for  $c \in \text{candidates}$  do
15:     if  $\text{CosineDistance}(x, c) \geq \tau$  then
16:        $\mathcal{D}_{test} \leftarrow \mathcal{D}_{test} \cup c$ 
17:     end if
18:   end for
19: end for
20: return  $\mathcal{D}_{train}, \mathcal{D}_{test}$ 
```

---

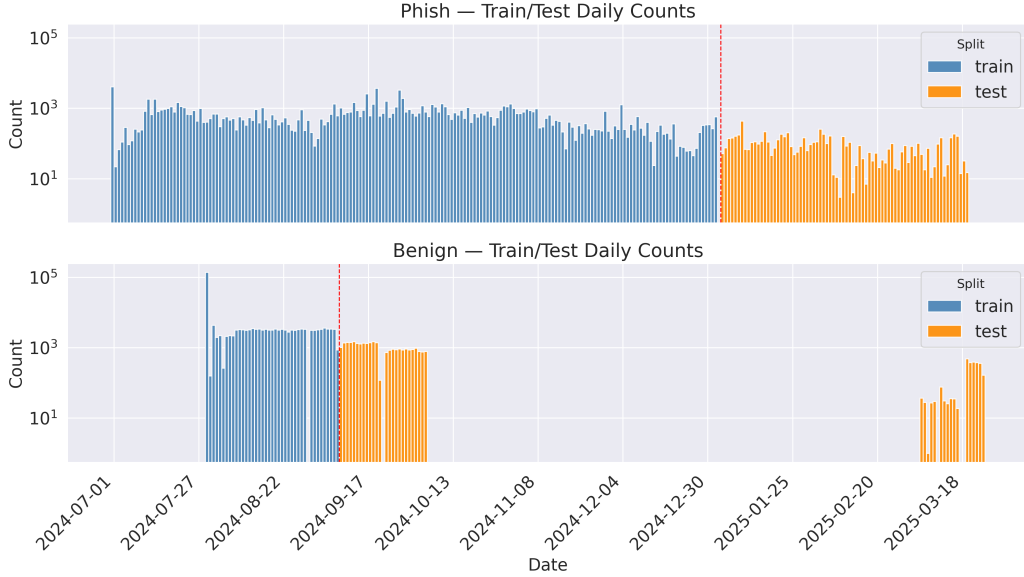


Figure 5: The train and test datasets are temporally disjoint for each class. Note: the benign test set shows a spike in the number of pages collected in March 2025; these are pages that were collected by scraping the Google search results of top targeted brands.

## E Baseline Experiments

### E.1 Setup, Hyperparameters and Training Details

The majority of experiments were performed on a single machine running Ubuntu 20.04 with an Intel Xeon Gold 6230 CPU and 4x NVIDIA V100 GPUs, each with 32 GB VRAM.

**Linear model** We implemented a linear support vector classifier (using LinearSVC) with squared hinge loss and L2 regularization. Key hyperparameters included: tolerance for convergence set to



---

**Algorithm 3** Benchmark dataset creation

---

```
1: Input:  $\mathcal{D}_{test}$  (test dataset),  $\mathcal{D}_{train}$  (train dataset)
2: Output:  $\mathcal{B}$  (benchmark datasets)
3:
4: // diversity enhancement
5:  $\mathcal{D}_{new} \leftarrow \mathcal{D}_{test} \cup \mathcal{D}_{targetBenign}$ 
6:  $\mathcal{D}_{new} \leftarrow \mathcal{D}_{new} \setminus \mathcal{D}_{similarHTML}$ 
7:
8: // difficulty filter
9:  $m \leftarrow \text{fitModel}(\mathcal{D}_{train})$ 
10:  $\text{score} \leftarrow m.\text{predict}(\mathcal{D}_{new})$ 
11:  $\mathcal{D}_{easy} \leftarrow \{x \mid \text{score}(x) > (1 - \delta) \wedge x \in P\} \cup \{x \mid \text{score}(x) < \delta \wedge x \in B\}$ 
12:  $\mathcal{D}_{discard} \leftarrow \text{sample}(k, \mathcal{D}_{easy})$ 
13:  $\mathcal{D}_{new} \leftarrow \mathcal{D}_{new} \setminus \mathcal{D}_{discard}$ 
14:
15: // base rate adjustment
16:  $\mathcal{D}_{benign} \leftarrow \{x \mid x \in \mathcal{D}_{new} \wedge x \in B\}$ 
17:  $\mathcal{D}_{phish} \leftarrow \{x \mid x \in \mathcal{D}_{new} \wedge x \in P\}$ 
18:  $\mathcal{B} \leftarrow \emptyset$ 
19: for  $b \in \{0.05, 0.1, 0.5, 1, 5\}$  do
20:    $\text{numPhish} \leftarrow \lfloor \frac{b \times |\mathcal{D}_{benign}|}{100 - b} \rfloor$ 
21:    $\text{numInstances} \leftarrow \text{getInstances}(b)$ 
22:    $\mathcal{D}'_{phish} \leftarrow \text{sample}(\mathcal{D}_{phish}, \text{numPhish}, \text{numInstances}, \text{replace} = \text{False})$ 
23:    $\mathcal{B} \leftarrow \mathcal{B} \cup \{\mathcal{D}_{benign}, \mathcal{D}'_{phish}\}$ 
24: end for
25: return  $\mathcal{B}$ 
```

---

$10^{-3}$ , dual set to `true` – due to large number of features, and `class_weight` set to ‘balanced’ – to weight samples inversely proportional to their class frequencies. The model used a combination of a few tens of hand-crafted features and a large number of n-gram features. The hand-crafted features included URL-based, such as the overall length of the URL, characteristics of the path, domain and subdomain structure, and lengths of individual components; and those derived from the HTML DOM structure, such as the number of nodes and edges in the DOM tree, to capture the structural complexity of the web page. The training converged in  $\sim 24$  epochs.

**FNN model** We used two types of n-gram features as input to our feedforward neural network (FNN) model. The first type consists of character-level 2-, 3-, and 4-grams extracted from the URL and selected sections of the parsed HTML, including: visible text, HTML tags, scripts, links, image sources, and embedded image data. The second type of n-gram feature is derived from XPath sequences extracted from the HTML DOM. Unlike the character-based n-grams, these XPath n-grams are computed at the tag level. For example, the 2-gram representation of the XPath sequence `<document>/<div>/<p>/<a>` includes the segments: `<document>/<div>`, `<div>/<p>`, and `<p>/<a>`. Each character-level or XPath n-gram is treated as an independent binary feature for input to the FNN.

The feature extraction process initially produced approximately 15.3 million binary features. We selected the 300,000 most frequent features from the training set for use in model training. Training was conducted over 10 epochs. The entire pipeline, including feature extraction and model training, completed in approximately 32 hours.

**BERT-based model** We fine-tuned `gpt-large` pre-trained embedding model on our training dataset using Hugging Face trainer with `adamw` optimizer, a learning rate of  $10^{-5}$ , momentum (`adam_beta1`) of 0.9 and a weight decay of  $10^{-4}$ . The model was fine-tuned for 2 epochs with `auto_find_batch_size` set to `true` for auto batch size discovery, which resulted in a batch size of 8 per device (32 in all). For the 2 epochs, it took about 27 hours.

**LLM-based prediction** We used OpenAI’s `gpt-4o-mini` model in batch mode to classify webpages as phishing or benign based on the input URL and HTML content. A system prompt was crafted to instruct the model to assess social engineering indicators and output a JSON containing two fields: a

phishing flag (boolean) and a phishing risk score (1–10). The HTML input is preprocessed to remove non-essential elements and truncated to stay within token limits. Each request includes the URL and simplified HTML in the prompt, and the model returns structured output used for phishing detection analysis. The token limit is set to 2500 for HTML and 500 for the prompt template. No token limit was imposed on the URL.

#### HTML simplification

To help shorten the input text, we remove unnecessary HTML elements such as metadata and styling. Following guidance from prior work in phishing detection using LLMs [26], the simplification process consists of: (1) Removing comments, `<style>`, and `<script>` tags; (2) Preserving content tags: `p`, `a`, `img`, `h1–h6`, `ul`, `ol`, `li`; (3) Filtering out tags with no text content; (4) Normalizing links and images by stripping `http(s)://` and `www.`; (5) If token limit is exceeded despite above steps, HTML elements are trimmed from the center until token limit is met.

#### System prompt

*"You are an expert in analyzing URLs and multilingual HTML to classify webpages as phishing or legitimate. Focus only on identifying whether the page is phishing and its corresponding risk score. First perform thorough reasoning on the URL and multi-lingual HTML and then classify with a confidence score. Given the following URL and HTML, analyze for social engineering techniques commonly used in phishing attacks: 1. PHISHING: Is the webpage phishing? (True if phishing, False otherwise) 2. SCORE: Phishing risk on a 1-10 scale (1 = least likely, 10 = most likely). Return the result in JSON format with the following fields: 'phishing': boolean, 'score': integer"*

## E.2 Evaluation results

Table 8 shows the mean average precision and the mean precision at recall = 0.9 of the four models on the test set (base rate: 18.3%)<sup>7</sup>. The 95% confidence intervals are computed based on 1000 stratified bootstrap samples on the test set.

Model		Test set (base rate: 18.3%)		
		Mean	Lower	Upper
Linear	AP	0.9815	0.9795	0.9835
	P@R = 0.90	0.9672	0.9596	0.9734
FNN	AP	0.9339	0.9296	0.9383
	P@R = 0.90	0.7991	0.7805	0.8141
GTE	AP	0.9918	0.9906	0.9929
	P@R = 0.90	0.9855	0.9825	0.9888
LLM	AP	0.8368	0.8280	0.8453
	P@R = 0.90	0.6930	0.6217	0.7771

Table 8: Mean average precision (AP) and precision at 90% recall for the test dataset, with the corresponding 95% confidence interval bounds provided in the 'Lower' and 'Upper' columns.

Next, we provide several visualizations to show the performance of the four models on the test and the benchmark datasets.

**Prediction Score Histograms** Figure 10 shows the score histogram for each of the models, with separate plots for benign and phishing points. The GTE model which has the best performance based on average precision also shows good class separation, with minimal overlap in the central score region. Further, the sharp peaks near zero and one, for the benign and phishing points, respectively, shows high confidence in correctly classified instances. Other models show multimodal distributions for the two classes, with lesser separation and greater overlap in the mid-score region.

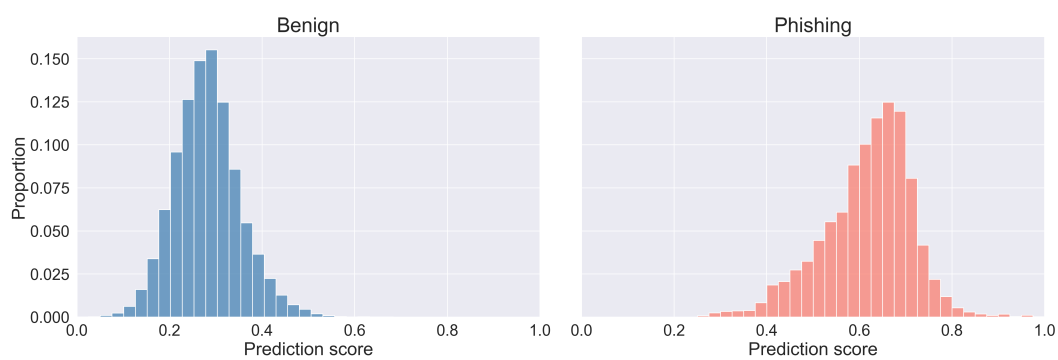
**ROC and PR curves** Figure 11 presents the ROC and precision-recall (PR) curves for the test dataset. Most models show strong performance, with the exception of the LLM-based model. The

<sup>7</sup>This is same as the last column of Table 2 but with confidence intervals added. The means here may not exactly match the ones in the other table since these were computed from bootstrap samples

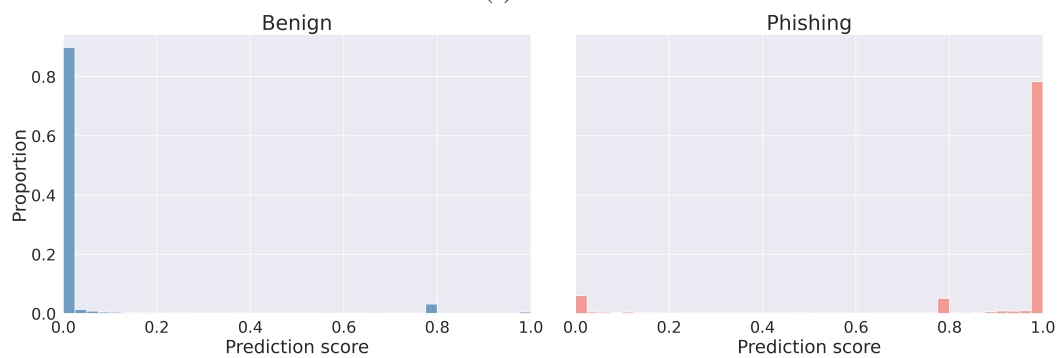
ROC-AUC values are quite close to 1.0, since the FPR values are numerically low, even at 18% base rate. As the base rate decreases, the FPP for a given level of precision tends to become even smaller. Consequently, we omit ROC curves for lower base rates.

**Confusion matrices** Figure 12 shows the trade off between precision and recall as the model threshold is changed. As the threshold increases the recall decreases while the precision increases. For example, at threshold of 0.7, the GTE model achieves a precision of 98.9% at a recall of 88%.

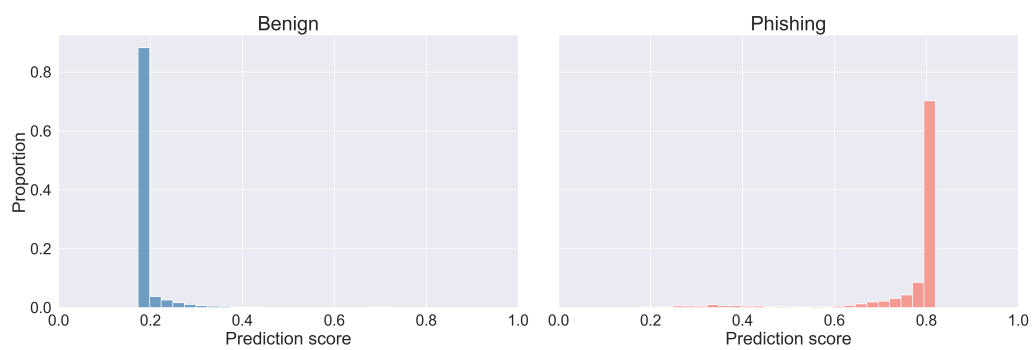
**PR curves on the Benchmark datasets** The precision-recall (PR) curves in Figure 13 show how the performance of the models decreases with decrease in base rate. Each plot presents five PR curves for each of the five base rates (0.05%, 0.1%, 0.5%, 1% and 5%).



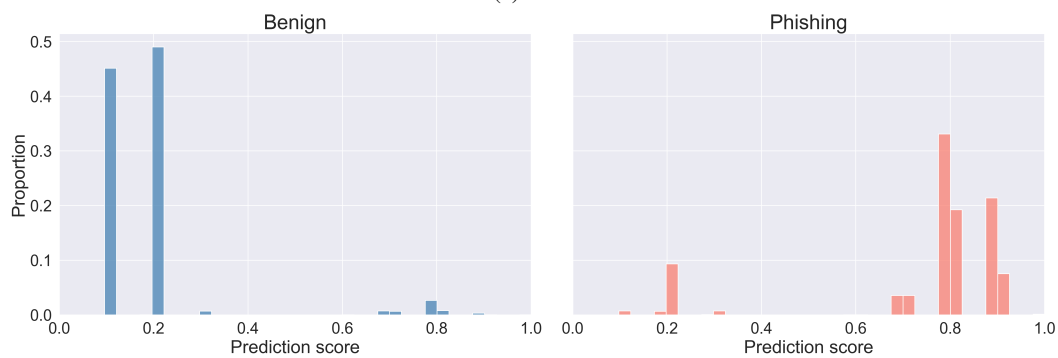
(a) Linear



(b) FNN

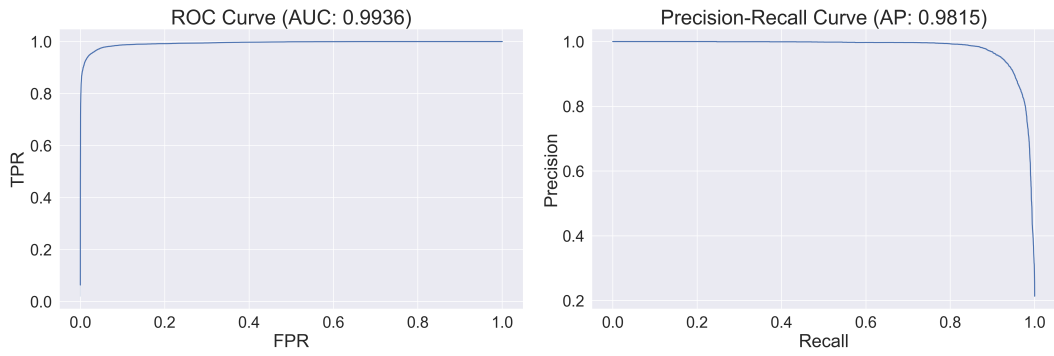


(c) GTE

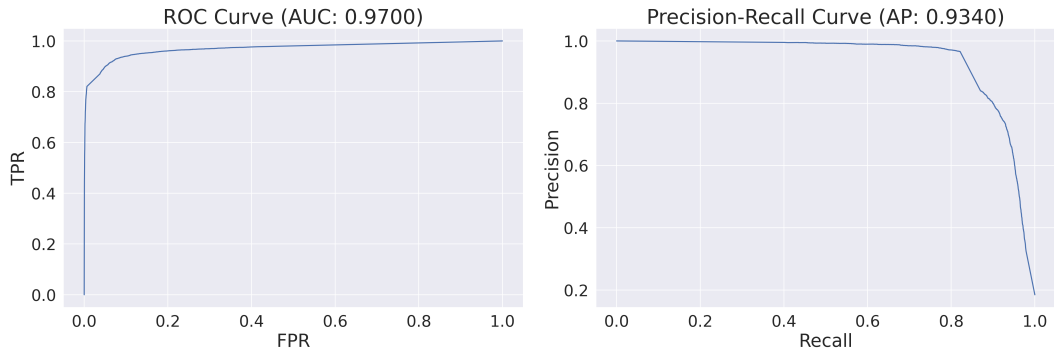


(d) LLM

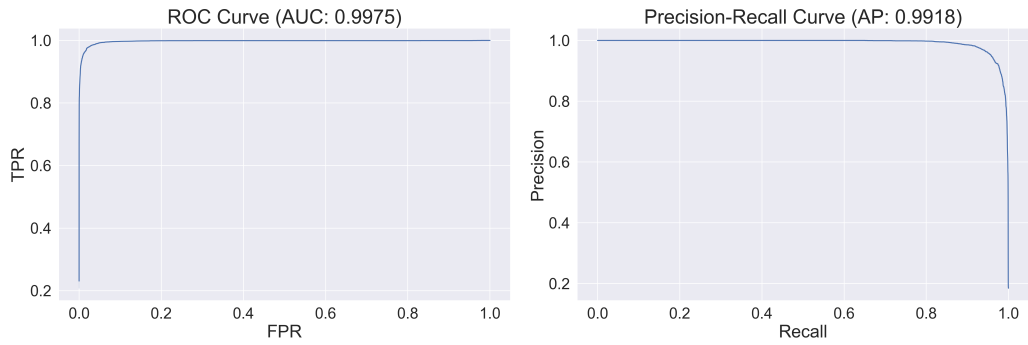
Figure 10: Model score distribution on the test dataset.



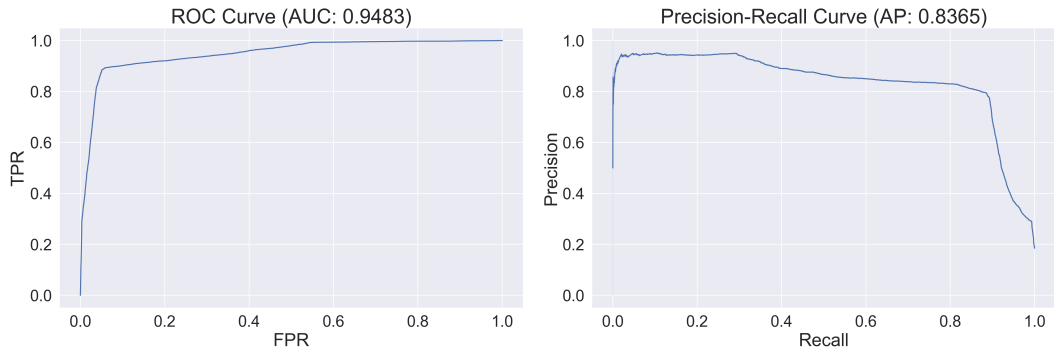
(a) Linear



(b) FNN



(c) GTE



(d) LLM

Figure 11: ROC and PR curves for the test dataset.

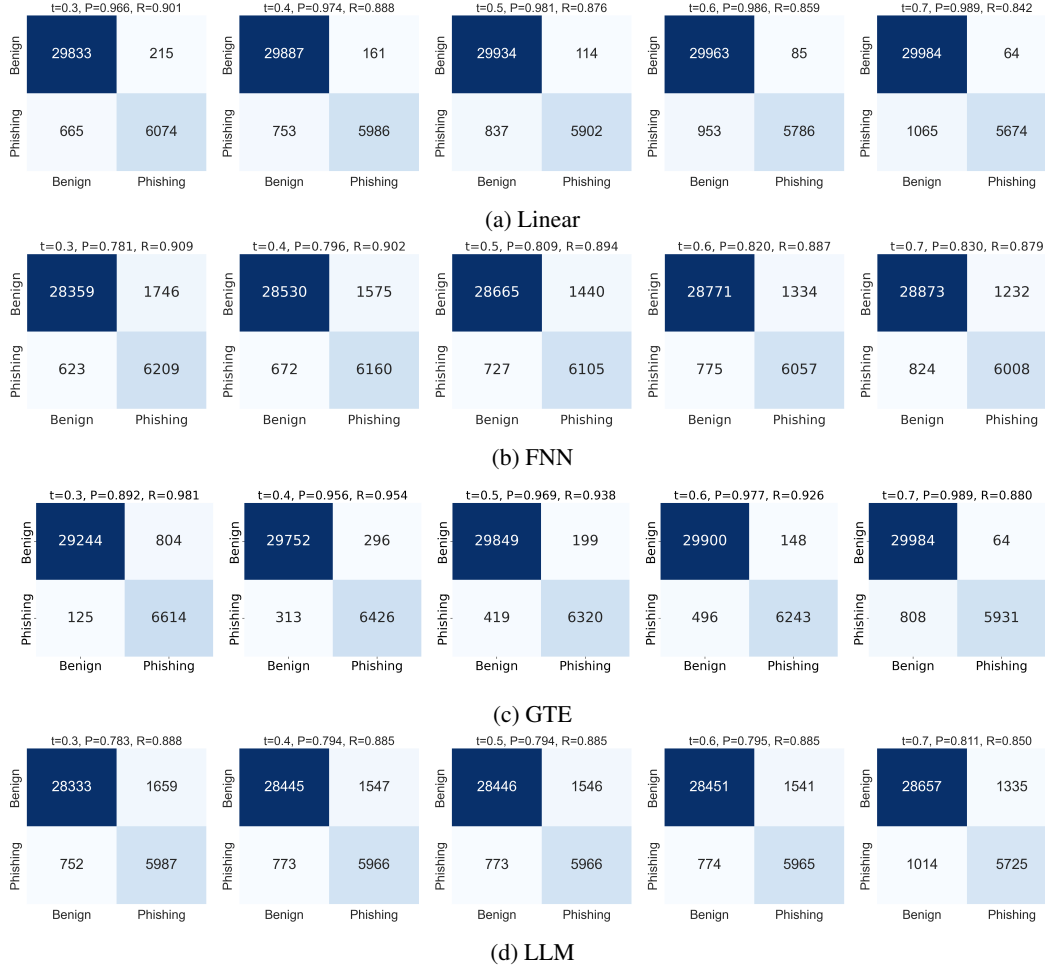
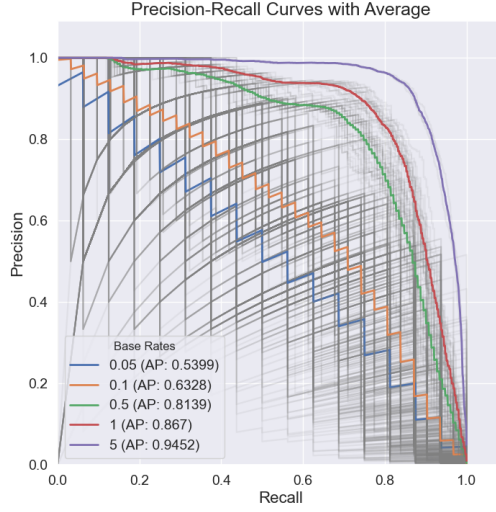
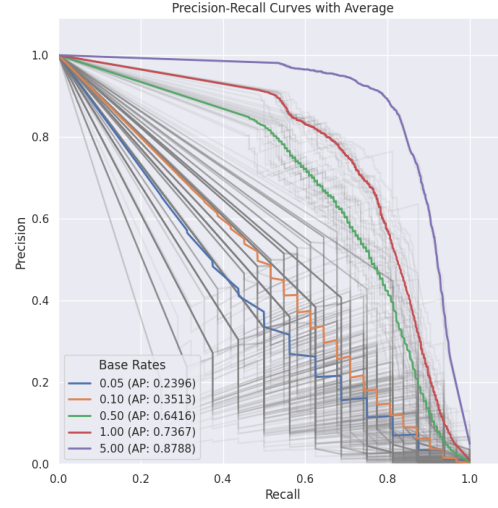


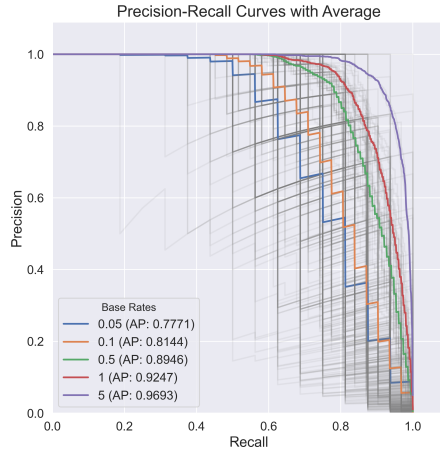
Figure 12: Confusion matrices at different thresholds (t) for the test dataset. In addition, the precision (P) and recall (R) at that threshold is also reported.



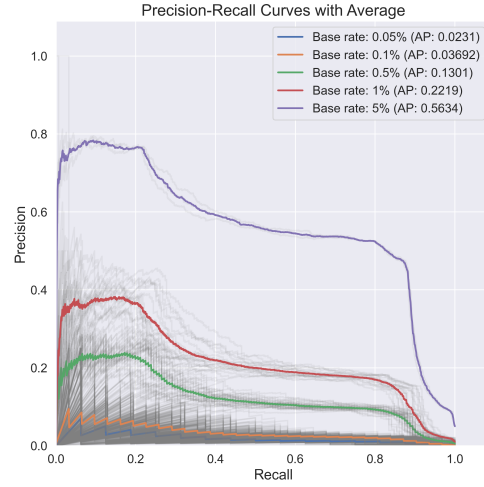
(a) Linear



(b) FNN



(c) GTE



(d) LLM

Figure 13: Precision-recall (PR) curves for the benchmark datasets are shown at five distinct base rates. For each base rate, the dark curve represents the average PR curve.